Chapter 4

NOVEL PHASE DIAGRAM OF A MIXED LANGMUIR MONOLAYER

4.1 Introduction

In this chapter we describe our studies on a mixed monolayer. Mixed monolayers are interesting for many reasons, *e.g.* they serve *e.g.* as membrane models [1]. Natural systems like lung surfactants are also mixed monolayers [2], though they are much more complex than the system studied here. It is possible to see the co-existence of more than two phases in a mixed monolayer. Our studies were conducted on a two component monolayer of 4′ - n - octyl - 4 - cyanobiphenyl (8CB) and stearic acid (SA) at room temperature. The molecular structures of the two compounds are given earlier. At room temperature the monolayer of 8CB shows the following phase sequence on compression

$$\text{Gas} \rightarrow \text{LE} \rightarrow \text{LE} + \text{D}_1 \rightarrow \text{LE} + \text{D}_1 + \text{D}_2$$

The phase diagram of fatty acid monolayers are described elaborately in Chapter 1. As mentioned there, they show a multitude of phases, depending on the chain length and temperature. In particular, for SA, the phases exhibited **[3]** at room temperature are:

$$\text{Gas} \rightarrow \text{L}_2 \rightarrow \text{LS} \rightarrow \text{collapsed state}.$$

The mixed monolayers of 8CB and SA have been studied by Enderle *et.al.* [1]

using surface manometry and second harmonic generation (SHG). They report a good mixing of the two species of molecules at high values of A.

We probed the mixed monolayer using epifluorescence microscopy in addition to surface manometry. Here, we could actually observe the phases being formed. The monolayer exhibited three – dimensional (3D) domains on compression, which we studied using reflection and polarising microscopy.

In the mixed monolayer, a liquid condensed (LC) phase was induced, which does not occur either for an 8CB or SA monolayer. This induction occurred over a large range of concentration (3% to 95% SA in 8CB). Also, for SA concentration between 55% and 95%, the familiar LE phase separated into two distinct phases, which we call the LE_1 and LE_2 phases. Of these, the LE_1 phase was 8CB rich while the LE_2 phase was SA rich. In addition, we also observed a three phase co-existence of the (i) gas, LE_1 and LE_2 and (ii) LE_1, LE_2 and LC phases. This three phase co-existence is permitted by Crisp's phase rule for 2D systems.

4.2 Experimental Techniques

The experimental techniques of surface manometry, fluorescence microscopy, reflection and polarising microscopy were employed to study the mixed monolayer. Stearic acid (SA) was obtained from Aldrich (USA) and used as received. Two dyes were used for epifluorescence studies, namely NBD-HDA and NBD octadecanoic acid (NBD-SA). Both the dyes were obtained from Molecular Probes, USA. The two dyes were used to rule out any possible artifacts arising due to a particular dye. The spreading solvent used here was chloroform of HPLC grade. Requisite solutions were prepared by mixing appropriate volumes from stock solutions of 8CB and SA using a Finpipette. The subphase, namely water was maintained at a constant temperature of 23 ± 1^{o}C.

Here we recall a few features associated with a dye doped monolayer under a fluorescence microscope. As mentioned in Chapter **2,** the gas phase appears dark and the LE phase appears bright. On compressing, the whole field of view

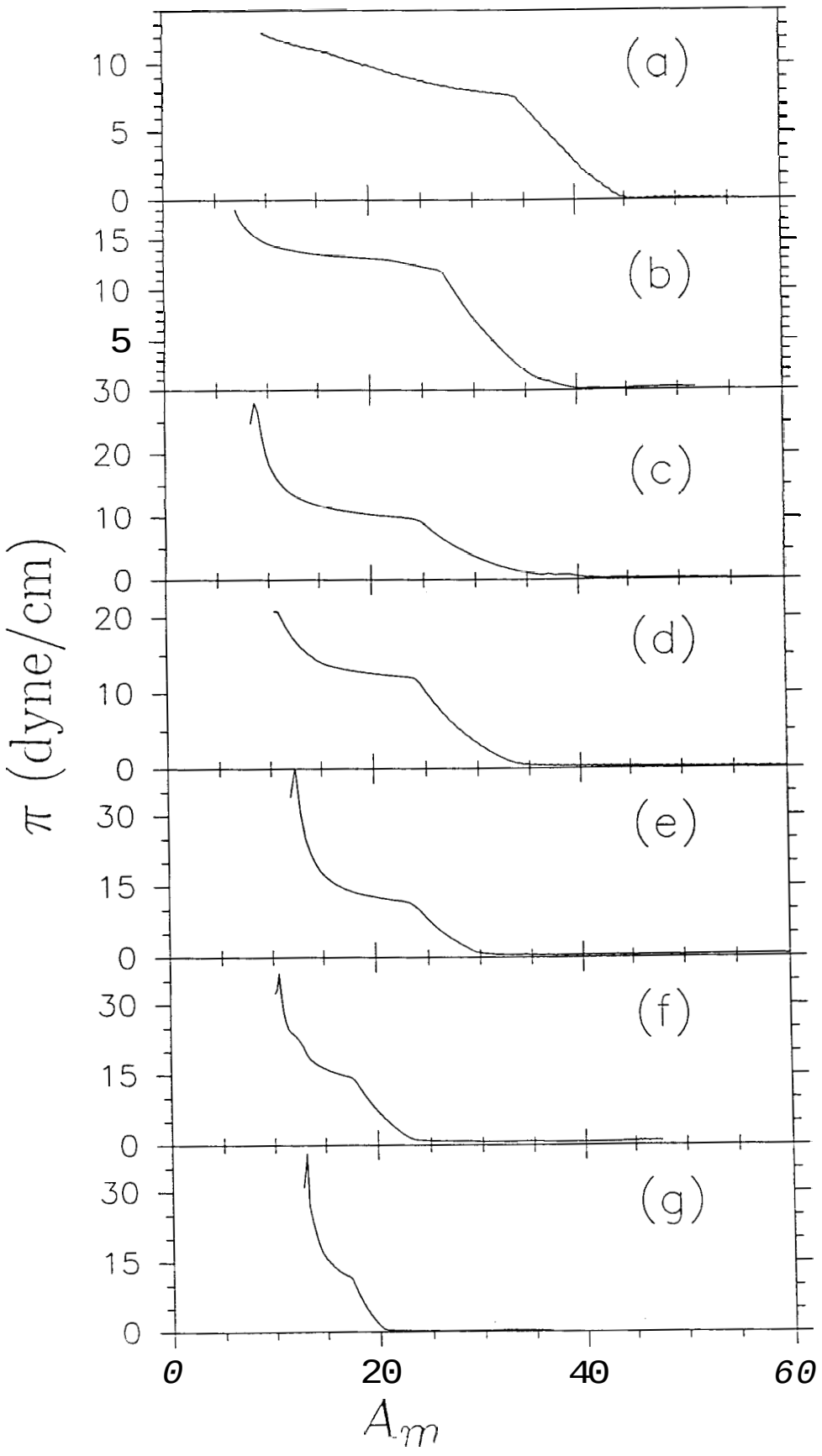

Figure 4.1 Surface Pressure isotherms for the mixed monolayers of 8CB and SA. The molecular concentrations of SA are (a) 15%, (b) 25%, (c) 50%, (d) 60%, (e) 75%, (f) 85%, and (g) 90%. The compression rate was 0.05 $Å^2$/molecule/second.

becomes uniformly bright, corresponding to the onset of the pure LE phase. On further compression, dark domains of the LC phase appear. These domains are dark due to expulsion of the dye from the LC phase [4].

4.3 Results

The π - A, isotherms for different molar concentrations of SA in 8CB are shown in Fig 4.1. The concentrations mentioned in this thesis are always molar concentrations. At high concentrations of SA, the isotherms resembled the isotherms of pure SA [1]. On the other hand, at high concentrations of 8CB, they resembled those of pure 8CB [Chapter 2]. The transition between the two extremes was smooth and continuous. This indicated a good mixing of the two species of molecules. This has also been reported for 8CB – pentadecanoic acid mixed monolayers [5]. The SA monolayer could be compressed to very high values of π (65 dyne/cm) before collapse. The surface pressure reduced as more and more 8CB was added. This could be due to the formation of three dimensional D_1 and D_2 (or D_3) domains in the 8CB rich monolayer. The formation of the 3D domains takes away molecules from the interface, thereby reducing $_{ri}$.

Based on these studies, we obtained the phase diagram shown in Fig 4.2. The important results are (i) the induction of the LC phase, (ii) the phase separation of the LE phase into LE_1 and LE_2 phases and (iii) the co-existence of three stable phases.

As shown in the phase diagram, there is a phase separation of the LE phase into two distinct phases, which we call the LE_1 and the LE_2 phases. Of these two phases, LE_1 is 8CB rich and LE_2 is SA rich. Also, there is an induction of the LC phase in the mixed monolayer, which does not occur for the monolayers of 8CB and SA. This induction occurs over almost the entire range of concentrations. In addition, there is a co-existence of three phases in a number of occasions.

The monolayer with SA upto **3%** in 8CB exhibited the phase sequence of pure 8CB. For a mixture with 15% SA in 8CB, there was the usual gas – LE_1

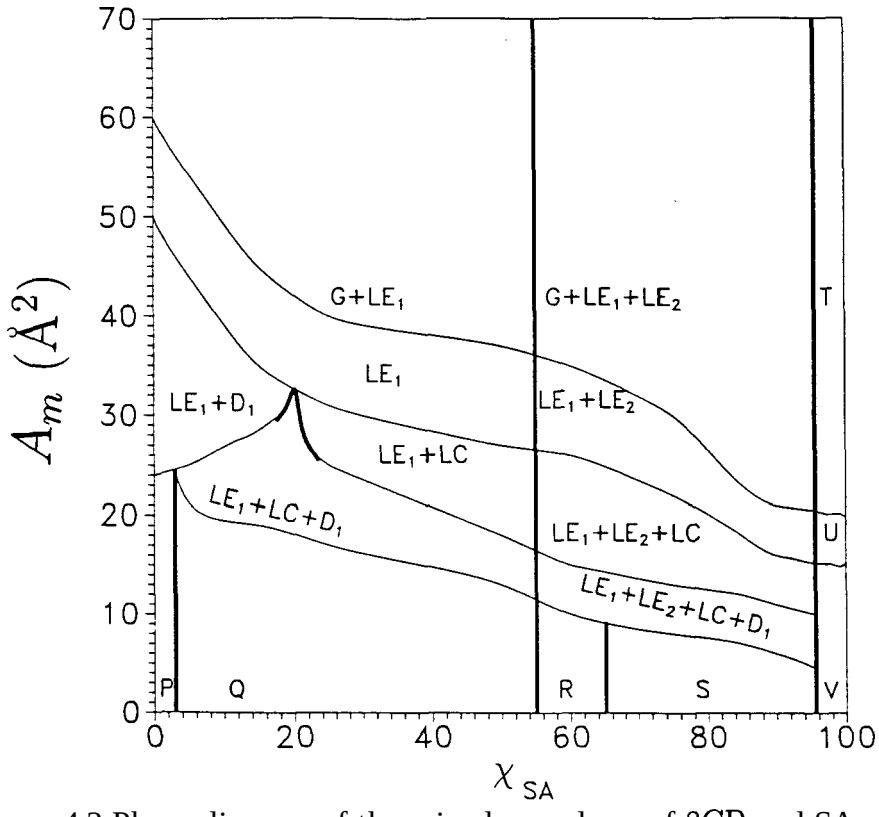

Figure 4.2 Phase diagram of the mixed monolayer of 8CB and SA at 23°C. [Key: P = LE_1+ D_1+ D_2, Q = LE_1+ LC + D_1+ D_2, R = LE_1+ LC + D_1+ D_3, S = LE_1+ LE_2+ LC + D_1+ D_3, T = gas + LE_2, U = LE_2, V = collapsed state.]

co-existence, followed by the LE_1 phase at 45Å^2 **A,.** On further compression, the D_1 domains appeared in the LE_1 phase, and grew at the expense of the LE_1 phase. This corresponded to the slope change in the isotherm at 35Å^2 **A,.** After this, dark LC domains started forming in the LE_1 – D_1 two phase mixture at 30 Å^2 **A,.** At this point, there was a slight change in the slope of the isotherm. Also, the monolayer started becoming less mobile from this point, as could be ascertained under the fluorescence microscope. Here the D_1 domains co-existed with the LE_1 and LC phases. Out of these, D_1 is an unstable structure. On further compression, the D_2 domains appeared. The D_2 domains were flat as they exhibited uniform colours under reflection. They were textureless under the polarising microscope, thereby indicating a smectic A ordering. This was further confirmed by using polarising microscopic studies of D_2 domains under convergent light. The behaviour of the monolayer was qualitatively similar for a concentration range of 3% to 20% SA in 8CB.

The behaviour of the monolayer with 25% SA in 8CB was not the same. Here

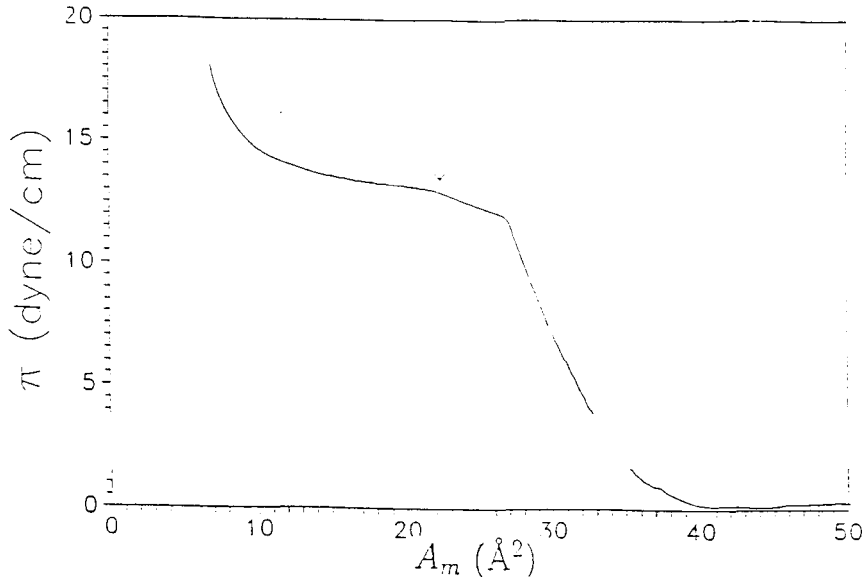

Figure 4.3 An enlarged plot of the isotherm for 25% SA in 8CB, shown in Fig 4.1(b). The change in slope marked by the arrow corresponds to the appearance of D_1 domains.

again the gas and LE_1 phases co-existed, which changed to the pure LE_1 phase on compression. On further compression, the LC phase appeared in the LE_1 phase at 27Å^2 A_m. The D_1 domains came later at 22Å^2 A_m. At this point, there is a clear change in the slope of the isotherm as indicated by an arrow in Fig 4.3. The LE_1, LC, D_1 co-existence is depicted in Fig 4.4. This was followed by the appearance of the D_2 domains. There was a co-existence of the LE_1, LC, D_1 and D_2 domains. This kind of behaviour persisted for a concentration range of 20% to 55% SA in 8CB.

The results for 60% SA in 8CB were very different. Here an SA rich LE_2 phase separated from the LE_1 phase. The phase sequence was:

$$\text{Gas} + LE_1 + LE_2 \rightarrow LE_1 + LE_2 \rightarrow LE_1 + LE_2 + LC \rightarrow LE_1 + LE_2 + LC + D_1 \rightarrow LE_1 + LE_2 + LC + D_1 + D_2.$$

The LE_2 phase was not as bright as the LE_1 phase, but was brighter than the gas phase. The three phases co-existed even for A, as high as 2008L^2. The

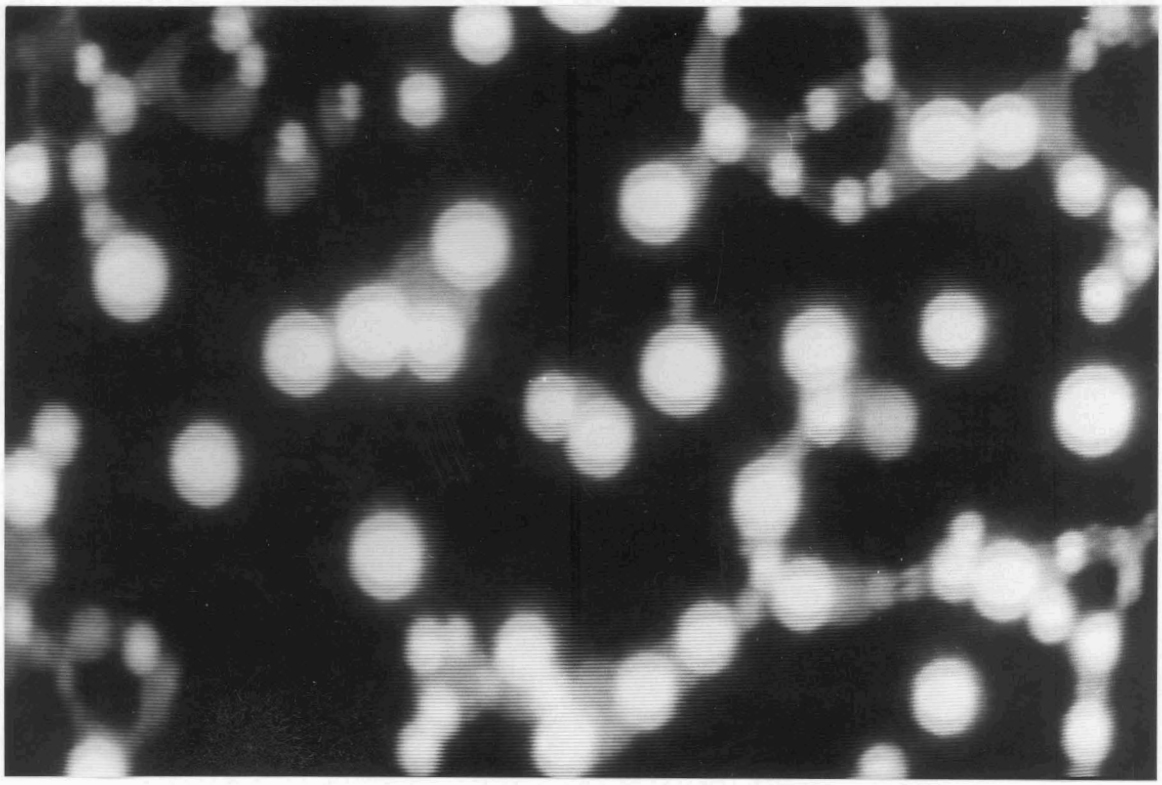

(a)

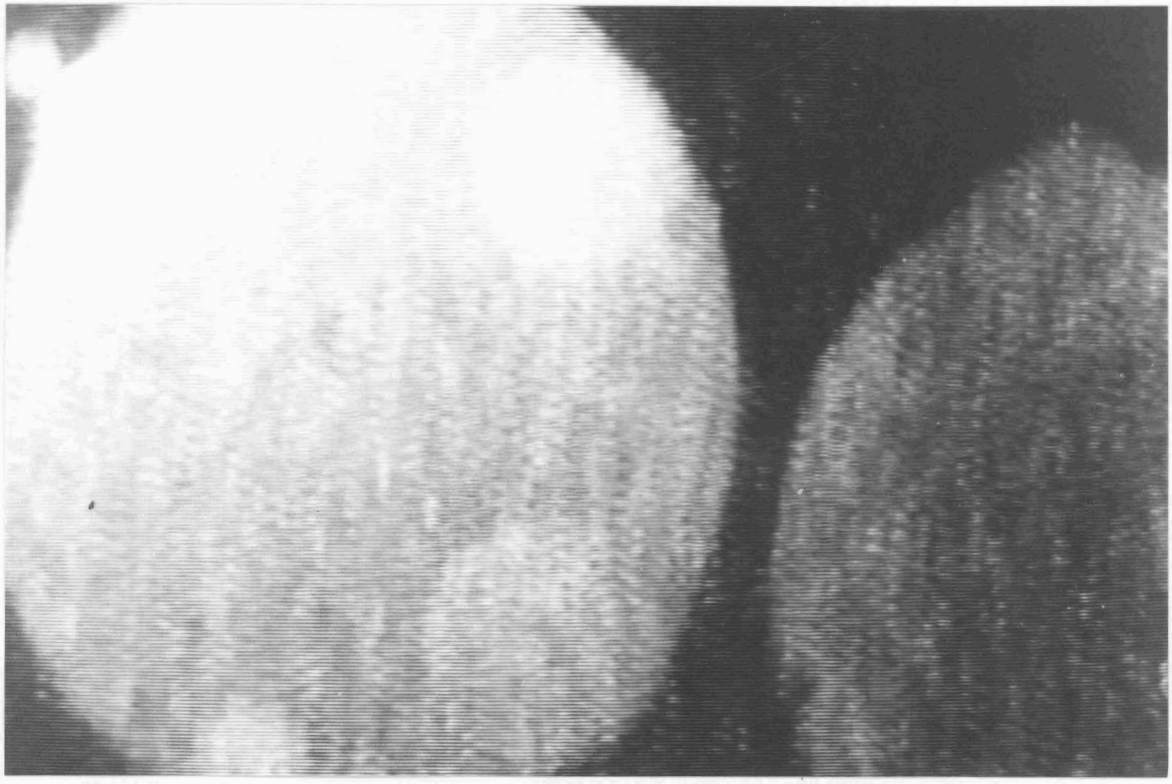

(b)

Figure 4.4 Fluorescence image of co-existing domains of D_1 (bright), LE_1 (grey) and LC (black) in the mixed monolayer of 25% SA in 8CB. (a) Small D_1 domains can be seen alongwith the LE_1 and LC phases. The image is taken at 25 $Å^2$ A, (b) D_1 domains growing near the edge of LE_1 phase. The image is taken at 30 $Å^2 A_m$. Scale of the images: 900μm x 600μM.

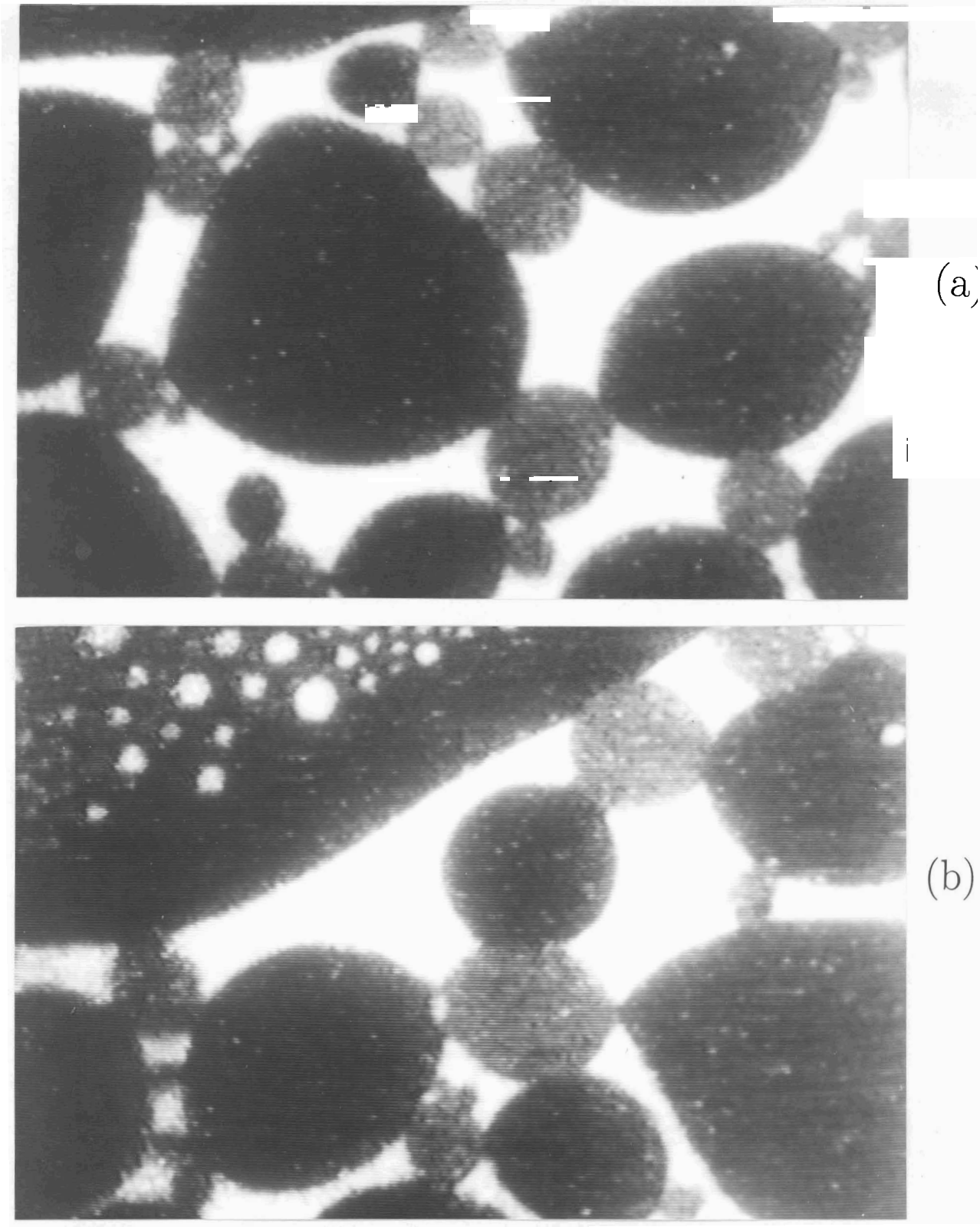

Figure 4.5 (a) Fluorescence image of co-existing LE_1 (bright), LE_2 (grey) and gas (black) phases. (b) Another image of LE_1, LE_2 gas co-existence. The molar concentration is 75% SA in 8CB. The images are taken at 50 $Å^2 A_m$. Scale of the images: 900 μm x 600 pm.

monolayer in the gas – LE_1 – LE_2 co-existence was as mobile as that in the gas – LE_1 co-existence seen so far. Fig 4.5 is a fluorescence image of the gas – LE_1 – LE_2 co-existence. On further compression, the gas phase disappeared and the monolayer exhibited a co-existence of LE_1 and LE_2 phases. On still further compression, the LC phase appeared. Here, the LE_1 and LE_2 phases co-existed with the LC phase, as shown in Fig 4.6. The mobility of the monolayer was much less in this three phase co-existence region. This phase sequence was seen for concentrations of SA between 55% and 65% in 8CB. It is interesting to note that here the LE_1, LE_2, LC, D_1 and D_2 phases co-existed.

The behaviour of the monolayer for concentrations between 65% and 95% SA in 8CB was similar, except that here D_3 domains appeared instead of the D_2 domains. The D_3 domains exhibited interference rings under reflection, indicating that they were lens like in shape. They showed distinct schlieren textures under the polarising microscope, indicating that they were in the nematic phase. Here the LE_1, LE_2, LC, D_1 and D_3 phases co-existed. Beyond this concentration, the monolayer behaved like that of pure SA. An interesting feature was that the isotherm for 85% molar concentration of SA in 8CB showed an extra plateau at 14 $Å^2$ ***A,.*** This plateau corresponded to the formation of D_1 domains, and was clear only for slow compressions at this molar concentration.

Under the fluorescence microscope, the D_1 domains appeared first in the LE_1 phase. The D_2 or D_3 domains appeared after that. In case of the LE_2 phase, generally the D_3 domains appeared directly. The D_1 domains appeared very rarely. Also, the appearance of the D_3 domains in the LE_2 phase was after the appearance of D_2 or D_3 domains in the LE_1 phase. The D_3 domains in the LE_2 phase were moving much more rapidly compared to those of similar size that grew in the LE_1 phase. This indicated more fluidity in the LE_2 phase as compared to the LE_1 phase. The epifluorescence experiments were repeated with two different dyes, NBD-HDA and NBD-SA. The sequence of phases and the relative areas occupied by the different phases were found to be identical, irrespective of the dye used.

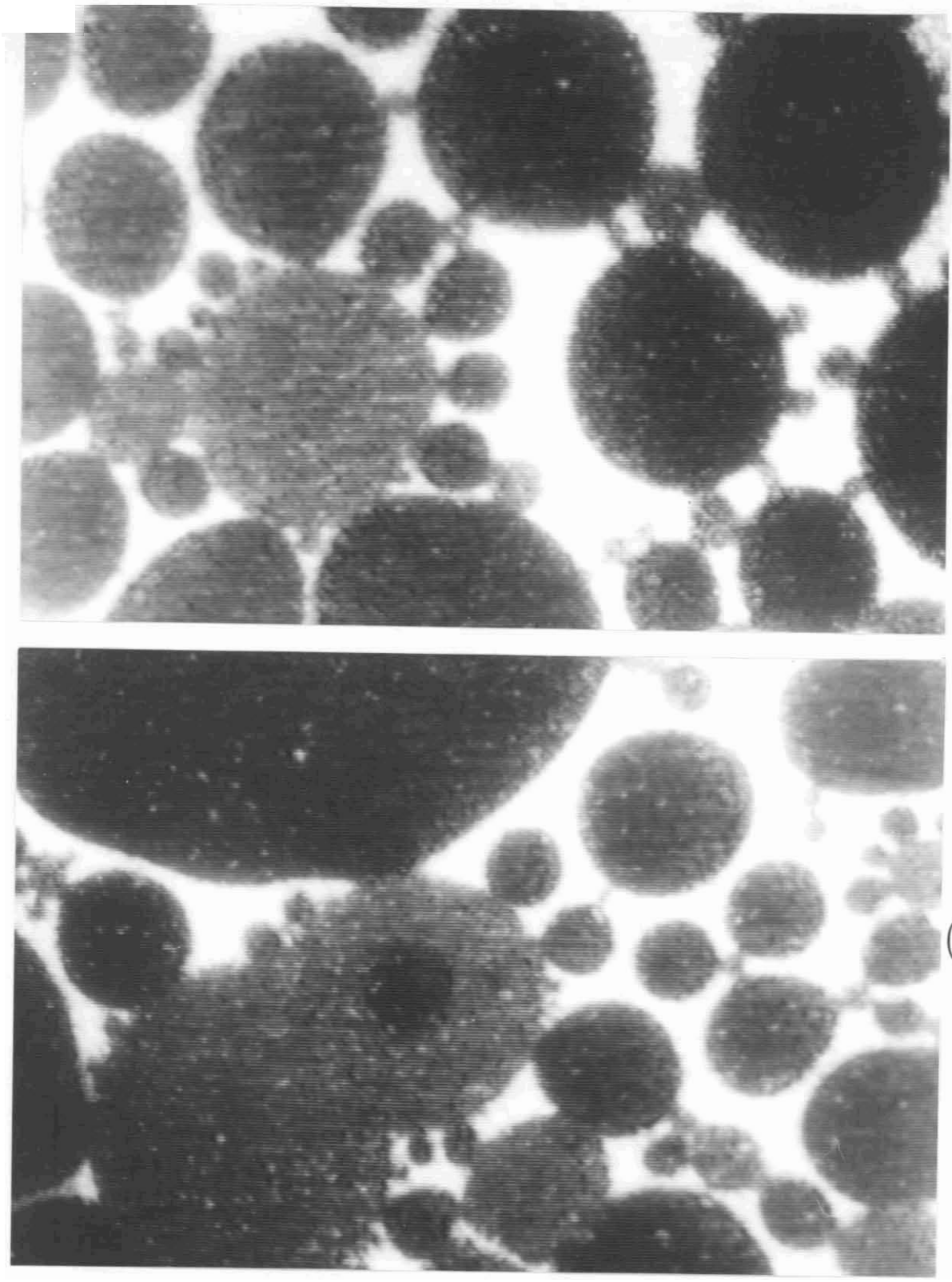

Figure 4.6 (a) Fluorescence image of co-existing domains of LE_1 (bright domains), LE_2 (grey) and LC (black) phases. (b) A similar image. An LC domain can be seen inside the LE_2 domain near the centre. The molar concentration is 75% SA in 8CB. The images are taken at 15 $Å^2 A_m$. Scale of the images: 900μm x 600μm.

Another interesting observation was that the area covered by the LE_2 phase increased with respect to that covered by the LE_1 phase as the SA concentration in the mixture was increased. At 60% SA concentration, the LE_2 phase was present only in traces, while at 90%, there was much more of LE_2 than LE_1.

4.4 Discussions

The results obtained from our studies on the mixed monolayer has a number of interesting implications. There is a steady decrease in the value of A, corresponding to the disappearance of the gas phase (Fig 4.2) as the SA concentration is increased. This can be interpreted to be due to the large size of the 8CB head group, which occupies more area at the interface, forcing the monolayer to condense into the liquid expanded phases.

4.4.1 Induced Liquid Condensed Phase

A very important result is the induction of the LC phase in the mixed monolayer. This phase does not appear in the monolayers of either 8CB or SA. This phase occurs for monolayers with a concentration of **3%** to 95% SA in 8CB. The induced phase appears dark under the fluorescence microscope due to expulsion of the dye, an indication of high density. Also, the monolayer becomes less mobile after this phase appears. Due to these reasons, we identify this phase as the LC phase. It might be the L_{2d}, the L_{2h} **[3]** or the fluid lamellar phase [6]. X-ray or miscibility studies are required to reveal the exact nature of the phase. Also, more information can be obtained by studying the monolayer by second harmonic generation, along with our results regarding phase co-existence and domain size. Dupin *et.al.* [7] have discussed the occurrence of liquid phases in fatty acid monolayers. They attribute the absence of two liquid phases in SA, unlike in the shorter chain myristic acid, to the long chain length of the SA molecules.

Ruckenstein and Li [8] have modelled the LE – LC phase transition for fatty acid monolayers. They consider the monolayer to be a 2D solution made up

of disordered molecules (DM), ordered molecules (OM) and clusters of ordered molecules. The OM are in all-trans configuration oriented normal to the interface, *i.e.* they are fully elongated (no kinks). The DM have at least one gauche defect in the hydrocarbon chain, *i.e.* there is a kink in the chain [9].

The LE – LC transition is due to DM changing to OM, and formation of clusters of OM. The DM act as a solvent for the OM clusters, which are the solutes. For the monolayer system, the chemical potentials can be written as

$$\mu_d = \mu_{od} + kTln(a_d) - \gamma A_{od} \tag{4.1}$$

for the DM and

$$\mu_i = \mu_{oi} + kTln(a_i) - \gamma A_o \qquad i = 1, 2, ..i_{max} \tag{4.2}$$

for clusters of OM having i molecules. In these equations, μ_o is the standard chemical potential, a is the activity and A_{od} and A_o are the A, values for the disordered and ordered molecules. **A,** is assumed to be a constant. i_{max} represents the number of molecules in the largest cluster, T is the temperature and γ is the surface tension.

The chemical potentials of DM and single OM (cluster of size $i = 1$) are equal at equilibrium. From this, the surface pressure is obtained as

$$\pi = \gamma_o + \frac{\mu_{o1} - \text{Pod}}{A_{od} - A_o} + \frac{kT}{A_{od} - A_o} ln\left(\frac{a_1}{a_d}\right) \tag{4.3}$$

Using the Florey – Huggins equation [10], the values of the activities are calculated to be

$$ln(a_d) = ln(\phi_d) + 1 - \frac{\phi_d}{x_d} + ln(\gamma_{rd}) \tag{4.4}$$

for the DM, and

$$ln(a_i) = ln(\phi_i) + 1 - \frac{\phi_i}{x_i} + ln(\gamma_{ri}) \qquad i = 1, 2, ..i_{max} \tag{4.5}$$

for OM clusters of size **i.** Here ϕ and x are the surface areas and the mole fractions respectively. The last terms in the two equations stand for the residual contribution resulting from mixing enthalpy of the solution.

For a noniconic surfactant like fatty acids, the following sources contribute to the change in the standard chemical potential $(\mu_{o1} - \mu_{od})$.

i). The change in the van der Waals interaction energy between the chains.

ii). The change in the head group steric interaction energy. This arises as the area occupied by a head group is excluded for the translational motion of the molecule at the interface.

iii). The change in the conformational free energy of the chains arises as the chains of the OM and DM are constrained to remain with the polar head groups in contact with water. This constraint affects the intramolecular interactions in the chains for OM and DM differently.

From this we obtain,

$$\frac{\mu_{o1} - \mu_{od}}{kT} = -\frac{}{1 - \left(\frac{A_o}{A_{od}}\right)^{1/2}} + ln\left[\left(\frac{A_{od} - A_p}{A. - A_p}\right)\left(\frac{A_o}{A_{od}}\right)\right] + \frac{2}{7}\frac{(n_c + 1)L^4}{(A_o)^2}\left[1 - \left(\frac{A_o}{A_{od}}\right)^2\right] \tag{4.6}$$

where **A,** is the effective cross section area of the carboxylic headgroup, L is the size of a segment which can be located on the lattice site **(4.6** Å) and n_c the no. of carbon atoms in the hydrocarbon chain.

The residual enthalpy (ΔH_{mix}) is calculated for a 2D lattice model representing the solution taking into account only nearest neighbour **(NN)** interactions. An OM occupies a single site surrounded by z_o NN. A DM or a cluster occupies more lattice sites, with a larger no of NN, z_d or z_i respectively.

Since only NN interactions are considered, only the interaction between the OM and DM contributes to the mixing enthalpy. Hence,

$$\frac{\Delta H_{mix}}{kT} = \left(\frac{A_{od}}{A_o}\right)^{1/2} N_d(1 - y_d)\chi \tag{4.7}$$

where $\chi = z_o \Delta W_{do}/kT$ is the interaction parameter between the OM and DM, N_d is the total no. of DM and y_d is the probability that a particular site is occupied by a DM. Based on this result, the activities become

$$ln(a_d) = ln(\phi_d) + 1 - \frac{\phi_d}{x_d} + \left(\frac{A_{od}}{A_o}\right)^{1/2} (1 - y_d)^2 \chi \tag{4.8}$$

for the DM, and

$$ln(a_i) = ln(\phi_i) + 1 - \frac{\phi_i}{x_i} + i^{1/2} y_d^2 \chi \quad i = 1, 2, ..i_{max} \tag{4.9}$$

for OM clusters of size i. The dispersive interaction energy based on van der Waal's interactions between two OM is given by [11]

$$W = \frac{W_o n_c}{32(A_o/3)^{5/2}} \tag{4.10}$$

for a hexagonal close packed lattice. Here $W_o = 8.62$ x 10^{-11} erg Å^5/molecule.

The interaction energy between two DM is considered to depend on their average height h_d. It is approximated to be the interaction energy between two OM with n_c corresponding to this height. Using this approximation, we get

$$W_{dd} = \frac{W_o A_o n_c / A_{od}}{32(A_o/3)^{5/2}} \tag{4.11}$$

From here we obtain

$$\chi = \frac{-z_o W_o n_c}{64kT(A_o/s)^{5/2}} [1 - (A_o/A_{od})^{1/2}]^2 \tag{4.12}$$

Based on all these results, the expression for surface pressure turns out to be

$$\begin{aligned} \frac{\pi(A_{od} - A_o)}{kT} &= \frac{\chi}{1 - \left(\frac{A_o}{A_{od}}\right)^{1/2}} + ln\left[\left(\frac{A_{od} - A_p}{A_o - A_p}\right)\left(\frac{A_o}{A_{od}}\right)\right] + \\ &\quad \frac{3}{7}\frac{(n_c + 1)L^4}{(A_o)^2}\left[1 - \left(\frac{A_o}{A_{od}}\right)^2\right] + ln\left(\frac{a_1}{a_d}\right) \end{aligned} \tag{4.13}$$

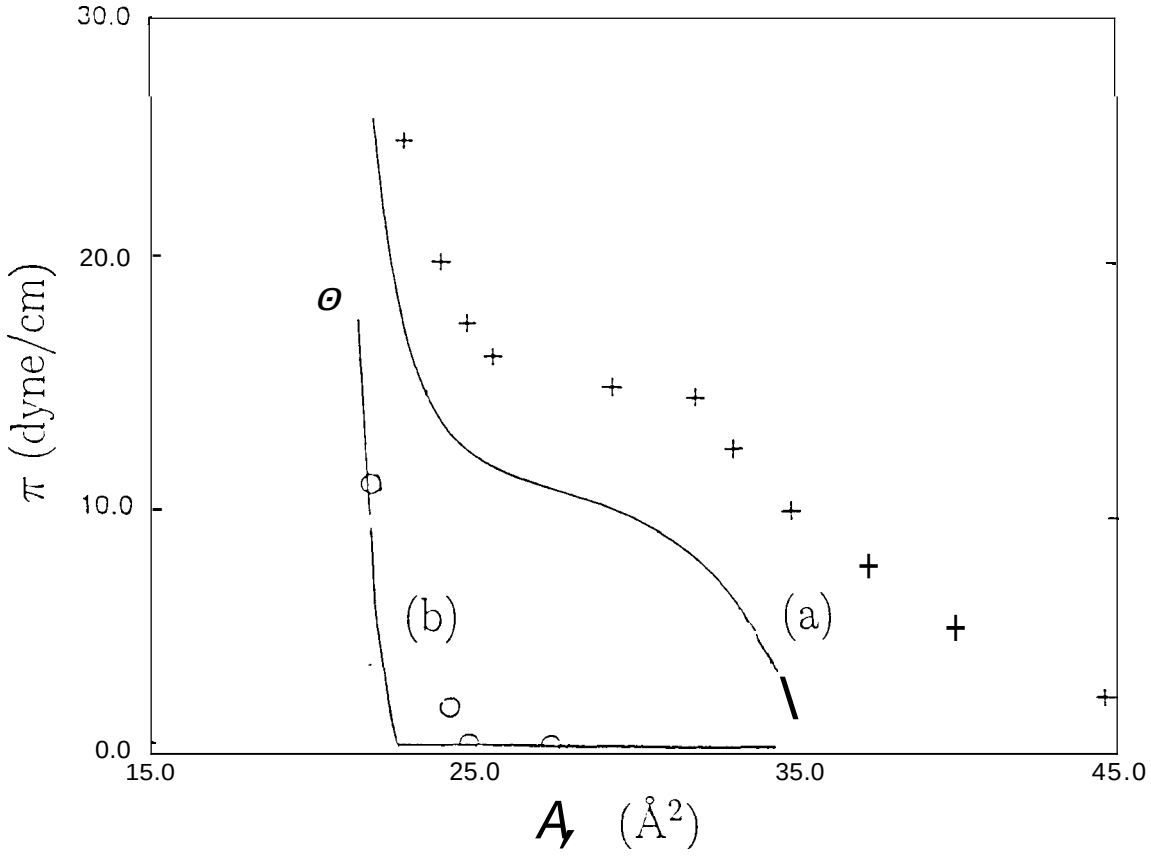

Figure **4.7** $\pi - A$, isotherms of two fatty acid monolayers. The symbols give the experimental results. The continuous lines are from the theory [8]. (a) The C_{14} (myristic) acid, and (b) The C_{17} (palmitic) acid

The $\pi - A$, isotherms of monolayers of C_{14} (myristic acid) and C_{17} (palmitic acid) fatty acids are shown in Fig **4.7.** The figure shows both the experimental results and the curves based on this model. As can be seen in the figure, the isotherm of C_{14} acid shows a distinct LE – LC phase transition. The isotherm is not horizontal in the two phase co-existence region. In case of the C_{17} acid, the isotherm does not exhibit any such transition. This indicates that the LE – LC transition is absent, as is expected for such long chain acids.

This theory can account for the induction of the LC phase. In the 8CB – SA mixed monolayer there could be a decrease in the effective chain length of the molecules due to the presence of the short 8CB molecules. This could lead to the induction of the LC phase. For mixed monolayers of fatty acids, the monolayer behaves like a monolayer of a fatty acid of an in between chain length [11].

Alternatively, it has been pointed out [12] that two liquid phases can be formed due to stiffness of the chains. Hence the 8CB molecules, whose chains are stiffer due to the presence of the biphenyl group, might be further aiding the formation

of the LC phase. We may also say that the effective anchoring at the water surface of the 8CB molecules is being increased by the presence of the COOH group of the SA molecules.

In this connection, another point to take note of is that for SA concentration 20% or less, the D_1 domains appeared before the LC phase. The order of appearance of the phases was reversed for a greater molar concentration of SA. This behaviour was obviously due to the subtle nature of the hydrophobic chain - subphase and polar headgroup - subphase interactions involved in the processes.

4.4.2 Phase Separation

Another very interesting new result of our experiment is the phase separation of the LE phase into the LE_1 and the LE_2 phases. Both the phases are highly mobile and the dye dissolves in them in the monolayer. Hence we broadly classify them as LE phases. The LE_1 phase has a smectic A like order and is definitely the L_1 phase. The LE_2 phase has a higher mobility than the LE_1 phase. It occurs for A, as high as 200 $Å^2$. Hence it is a low density phase. This can also be suggested from the fact that the dye is soluble in this phase. So, the LE_2 phase is likely to be a modified form of the L_1 phase. These two phases are distinct, as indicated by the clear phase separation. Such a phase separation has not been reported in the literature to our knowledge. To confirm that the phase separation is not induced by a particular dye, we repeated the experiments with two different dyes. The phase separation and relative areas occupied by the LE_1 and LE_2 phases do not depend on the particular dye used, indicating that it is a true phase separation. It would be useful to study these phases using X-ray diffraction for detailed structural identification of the phases. Also, atomic force microscopy and x-ray diffraction of the monolayer, after transferring it onto a solid substrate by LB technique might provide useful information.

The LE_1 and LE_2 phases appear only after SA concentration is increased to 55%. Until this concentration is reached, there is only the LE phase (which we call LE_1) in the monolayer. As the SA concentration is increased further,

the LE_2 phase increases in area at the expense of the LE_1 phase. Also, the D_1 domains, which are characteristic of a pure 8CB monolayer, appear first in the LE_1 phase. In addition, the LE_1 phase has a lower fluidity than the LE_2 phase. This indicates a higher proportion of 8CB as the larger headgroup of 8CB can impede movement. Based on these results, we conclude that the LE_1 phase is 8CB rich while the LE_2 phase is SA rich. It would be very interesting to probe the actual 8CB SA ratio in the LE_1 and LE_2 phases. This may throw some light on the mechanism of the phase separation and also tell about the behaviour of the two species of molecules.

Pan and Toxvaerd [13] have studied 2D binary fluids comprising of different sized molecules under a Lennard – Jones potential by molecular dynamics simulation. They report a phase separation of the two species of molecules. Such a mechanism may also be responsible for the phase separation of the LE phase in the 8CB – SA mixed monolayer.

4.4.3 Three Phase Co-existence

A significant result of our thesis is the co-existence of three phase, namely (i) gas, LE_1 and LE_2 (see Fig 4.5) and (ii) LE_1, LE_2 and LC (see Fig 4.6). The three phase co-existence can be accounted for by the application of Crisp's phase rule [14] for 2D systems. If we consider a 2D film separated by two bulk phases at any temperature and pressure, the no. of degrees of freedom (f) for the film is given by

$$f = C^B + C^S - P^B - q + 3 \tag{4.14}$$

where C^B = total no. of components in the bulk phases;

C^S = no. of components in the monolayer at the interface;

P^B = total no. of bulk phases separated by the interface;

q = total no. of phases in the monolayer.

If the temperature and pressure be fixed, the equation reduces to

$$f = C^B + C^S - P^B - q + 1 \tag{4.15}$$

For our system, $C^B = 2$ (air and water), $C^S = 2$ (8CB and SA) and $P^B = 2$ (gas and liquid). So equation 2 gives

$$f = 3 - q \tag{4.16}$$

Thus, a two component monolayer can have a co-existence of a maximum of three stable phases. At first, our experimental observation, namely the co-existence of LE_1, LE_2, LC, D_1 and D_3 phases, might appear to contradict this result. But, this is possible because the D_1, D_2 and D_3 phases are 3D structures and hence the Crisp's phase rule is not applicable to them.

4.4.4 Domain Shapes

A point to be noted is that flat D_2 domains occur for SA concentrations upto *55%* and lens shaped D_3 domains for higher concentrations. As described in Chapter **2,** for pure 8CB only D_2 domains are formed at 23°C. The D_3 domains appear above 28°C, when 8CB is in the nematic phase. Hence, we infer that the presence of a large amount of SA in the vicinity is lowering the smectic A - nematic transition temperature to sub-ambient levels once the SA concentration is more than *55%.* As such the mixture is in the nematic phase giving rise to D_3 domains with nematic order. Under the polarising microscope, schlieren texture is seen in these domains, confirming that they are in nematic phase. The fact that D_1 domains are rarely seen in the LE_2 phase may also be due to the same reason. Here, due to the very high SA concentration, the mixture may be in the isotropic phase where the D_1 domains do not occur.

4.4.5 Squeezing Out of 8CB from the Interface

At high surface density, some D_2 domains appear to enter into the LC areas of the monolayer. In such cases, the LC domains look like dark crescents. This is shown

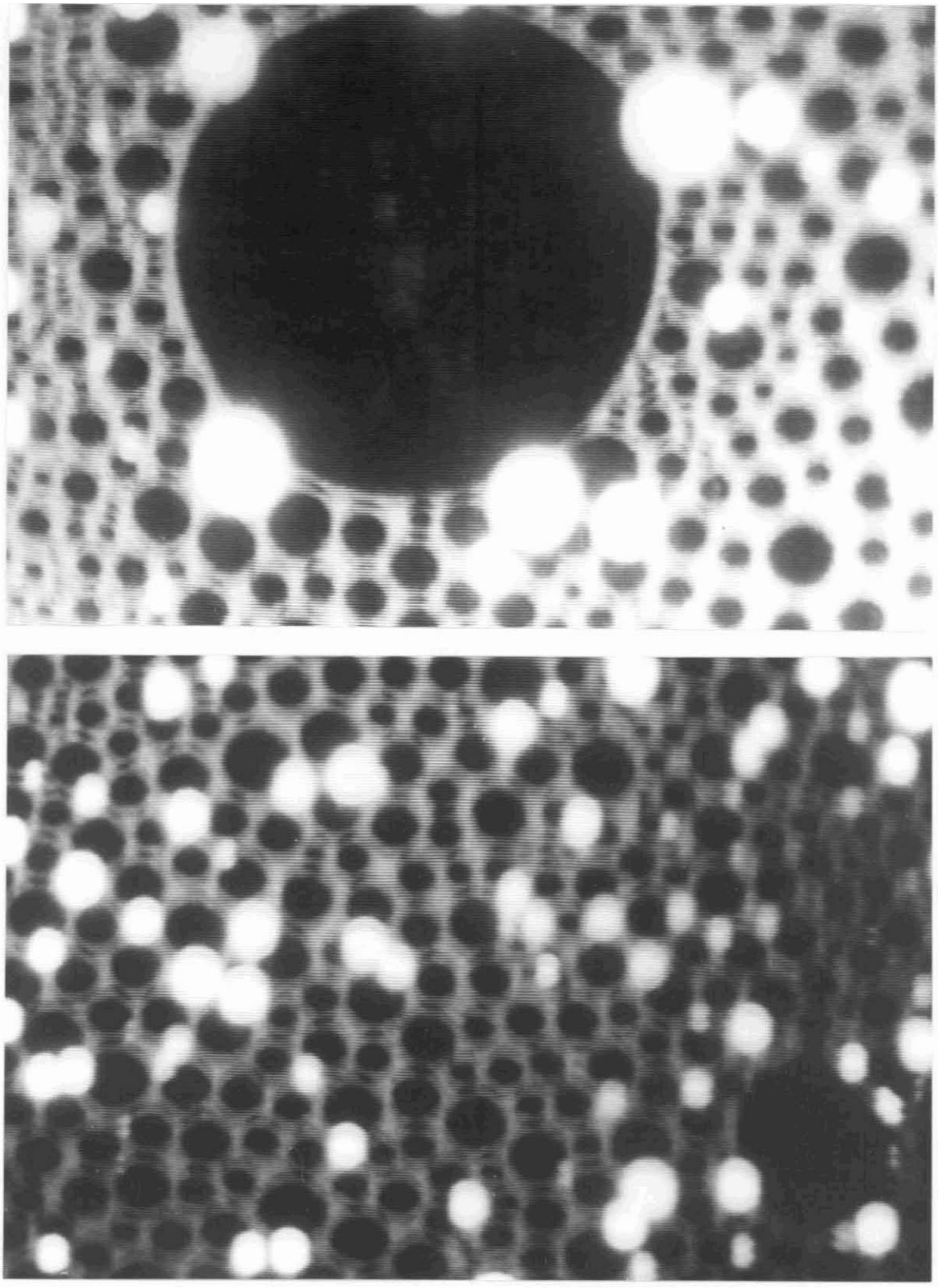

Figure 4.8 Fluorescence image of D_2 domains (bright) co-existing with LE_1 (grey) and LC (black) phases. (a) Four D_2 domains entering into a large LC domain. (b) Small D_2 domains entering the LC domains, making the LC domains appear as black crescents. The grey background consists of LE_1 and D_1 domains. Molar concentration is 25% SA in 8CB, at $10 Å^2 A_m$. Scale of the images: $900\mu m$ x $600\mu m$.

in Fig 4.8. This may be due to the expulsion of 8CB molecules from the interface. These expelled molecules form a D_2 domain over the monolayer. According to Enderle *et.al.* [1], all the 8CB molecules are expelled from the monolayer on compression and they settle over the SA monolayer. If there is such a total expulsion of 8CB molecules, the A_s value at the peak surface pressure should go on decreasing as more and more 8CB is added, as it effectively becomes an SA monolayer with less number of molecules. The expelled 8CB molecules are not at the interface and so should not affect the monolayer properties at all. As can be seen in Fig 4.1, there is no such trend. Also, the π value at the onset of collapse for the mixed monolayer is less than that for the pure SA monolayer. This again indicates that at least some 8CB molecules are at the interface. So, we suggest that there is a partial seggregation of the 8CB molecules. This result is in agreement with the results on 8CB-pentadecanoic acid mixed monolayers [5].

Fang and Uphaus [15] have studied a mixed monolayer of a nematic liquid crystal and stearic acid by surface manometry and x-ray studies of the corresponding LB films. They also observe a squeezing out of the liquid crystalline molecule at high surface density. However, they expect the liquid crystalline molecule to be pulled into the subphase, instead of being pushed out. In their case, the liquid crystal molecule has a shorter chain length and a strong hydrophobic group compared to SA.

A thermodynamic model proposed by Enderle *et.al.* [1] attempts to evaluate the critical value of π at which the 8CB molecules start leaving the interface. They consider the system to be a mixed monolayer of 8CB and SA with a bulk phase of 8CB resting over it. In thermodynamic equilibrium, the 8CB molecules can move between the two, while the SA molecules are rooted to the water surface due to their stronger hydrophilic attraction. The bulk phase serves as a particle bath for the 8CB molecules.

The 8CB and SA molecules are considered hard spheres with cross section areas A^*_{8CB} or A^*_{SA} respectively. The strength of the interaction with water for each

species is accounted for by fixing the maximum surface pressure upto which the molecules stay at the interface. There are no interactions between the molecules except collisions. At thermodynamic equilibrium, only the 8CB molecules can move between the two phases. Based on these assumptions, the authors calculate the critical value of π where the 8CB molecules start leaving the interface as

$$\pi^*_{mix} = \pi^*_{8CB} - \frac{NkT(1-\chi_{SA}).ln(1-\chi_{SA})}{\chi_{SA}A^*_{SAm} + (1-\chi_{SA})A^*_{8CBm}}. \tag{4.17}$$

where $\pi^*_{8CB} = \pi$ value corresponding to the formation of D_1 domains in pure 8CB monolyer and χ_{SA} = mole fraction of SA. Fitting this equation to the experimentally obtained values, the authors obtain $\pi^*_{8CB} = 6.4$ dyne/cm, $A^*_{8CBm} = 42.0$ Å^2 and $A^*_{SAm} = 20.3$ Å^2. These values agree with the experimental values for the monolayers of 8CB and SA.

However, our results are different from the results of Enderle *et.al.* [1]. They speculate a total squeezing out of 8CB molecules from the surface. We believe that the squeezing of 8CB molecules is partial.

Our phase diagram studies of the mixed monolayers of SA and 8CB show new phases and co-existence of different phases. This should lead to a better understanding of the formation of the LB films of these materials. It is well known that SA is one of the best LB materials. However, it is difficult to transfer it in a pure form [3], and it is transferred in the form of a salt. Our studies may be useful for preparing good LB films for industrial applications.

4.5 Conclusions

The mixed monolayer of 8CB and SA behaves differently from the monolayers of either component. The system shows the induction of a new phase. This induced phase is dense and has a lower mobility compared to the liquid expanded phases, hence it is identified as the liquid condensed phase. The induction appears to be due to the effective reduction of hydrophobic chain length of SA due to the presence of the 8CB molecules, along with an increase in the chain stiffness. On

the basis of a model of the LE – LC phase transition by Ruckenstein and Li [8], we suggest that this induction is likely to be due to the reduction of the effective chain length. Alternatively, it may be said to be due to an effective increase of the hydrophilic anchoring of the 8CB molecules due to the presence of the SA molecules.

There is a phase separation of the LE phase into 8CB rich LE_1 and SA rich LE_2 phases. These phases are distinct and exhibit different intensities under the fluorescence microscope. Both the phases are highly mobile, suggesting that they are liquid expanded phases. This phase separation occurs over a wide range of concentrations, from 55% to 95% SA in 8CB.

The mixed monolayer exhibits a co-existence of three phases, namely *(i)* LE_1, LE_2 and gas and *(ii)* LE_1, LE_2 and LC phases. This three – phase co-existence is in agreement with the 2D phase rule by D. J. Crisp [14].

The shape of the 3D domains depend on the concentration of SA in the mixed monolayer. This is due to the impurity effect which tends to reduce the transition temperatures of the mixed system. We have confirmed by polarising microscope studies that the transition temperatures are lowered.

Bibliography

[1] Th. Enderle, A. J. Meixner and I. Zschokke-Granacher, J. Chem. Phys., 101, 4365 (1994).

[2] M. M. Lipp, K. Y. C. Lee, J. A. Zasadzinski and A. J. Waig, Science, 273, 1196 (1990).

[3] A. M. Bibo and I. R. Peterson, Adv. Muter., 2, 309 (1990).

[4] X. Qiu, J. Ruiz-Garcia, K. J. Stine, C. M. Knobler and J. V. Selinger, Phys. Rev. Lett., 67, 703 (1991).

[5] M. Barmentlo and Q. H. F. Vrehen, Chem. Phys. Lett., 209, 347, (1993).

[6] O. Albrecht, H. Gruler and E. Sackmann, J. de Physique, 39, 301 (1978).

[7] J. J. Dupin. J. L. Firpo, G. Albinet, A. G. Bois, L. Casalla and J. F. Baret, J. Chem. Phys., 70, 2357, (1979).

[8] E. Ruckenstein and B. Li, J. Phys. Chem., 100, 3108 (1996)

[9] A. Ulman, An Introduction to Ultrathin Organic Films (Academic Press), (1991).

[10] U. V. Gedde, Polymer Physics, (Chapman and Hall) (1995).

[11] K. S. Birdi, Lipid and *Biopolymer* Monolayers at Liquid Interfaces, (Plenum Press) (1989).

[12] F. Schmid and M. Schick, J. Chem. Phys., 102, 2080 (1995).

[13] L. Pan and S. Toxvaerd, Phys. Rev. E, 54, 6532 (1996)

[14] D. J. Crisp, Surface Chemistry Suppl. Research, Butterworths, London (1949), pp17, 23.

[15] J. Y. Fang and R. A. Uphaus, Langmuir, 10, 1005 (1994).